JOC The Journal of Organic Chemistry

pubs.acs.org/joc Article

Copper-Mediated Single-Electron Approach to Indoline Amination: Scope, Mechanism, and Total Synthesis of Asperazine A

James B. Shaum, Andrei Nikolaev, Helena C. Steffens, Luis Gonzalez, Shamon Walker, Andrey V. Samoshin, Gabrielle Hammersley, Ellia H. La, and Javier Read de Alaniz*

Cite This: J. Org. Chem. 2022, 87, 9907−9914 Read Online

ABSTRACT: Pyrroloindolines bearing a C3−N linkage comprise the core of many biologically active natural products, but many methods toward their synthesis are limited by the sterics or electronics of the product. We report a single electron-based approach for the synthesis of this scaffold and demonstrate high-yielding aminations, regardless of electronic or steric demands. The transformation uses copper wire and isopropanol to promote the reaction. The broad synthetic utility of this heterogeneous copper-catalyzed approach to access pyrroloindolines, diketopiperazine, furoindoline, and (+)-asperazine is included, along with experiments to provide insight into the mechanism of this new process.

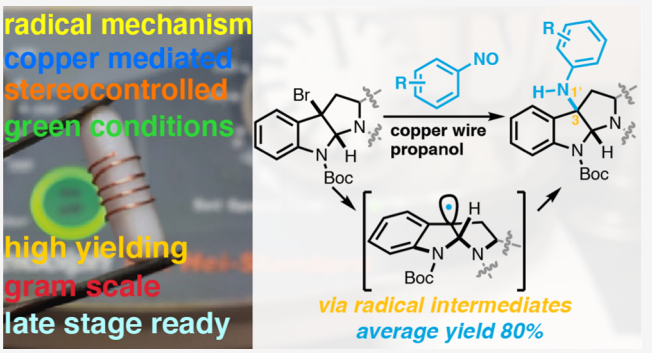

INTRODUCTION

Pyrroloindolines constitute the core of many cytotoxic natural products isolated from marine and terrestrial fungi as well as the rubiaceous cousins of the coffee plant. This class of indole alkaloids has been a perennial target for organic chemists, owing to their biological activities, as well as the molecule's complex structures.[1−4] Pyrroloindoline natural products bearing a C3−N1′ bond, such as asperazine A and pestalazine B (Scheme 1A), are particularly attractive targets owing to the unique challenge of installing the C3−N indoline linkage and their anticancer and antibiotic properties.[2,3] Further, these natural products and their C3−N1′ linkage have seen significantly less investigation from the synthetic community than natural products containing a C3−C bond, such as asperazine, pestalazine A, and many others.

In general, the majority of methods fall into one of two strategic disconnections to construct the pyrroloindoline motif bearing a C3−N1′ bond. One of the most widely adopted strategies commences from tryptamine and tryptophan scaffolds and occurs through direct C3−nitrogen functionalization followed by cyclization of a pendant nucleophile onto the resulting iminium ion. Some notable examples of this approach include Baran's electrophilic amination with *ortho*-iodoaniline to access psychotrimine efficiently,[5−7] Knowles' photo-iridium driven enantioselective synthesis,[8] Deng's copper-catalyzed nitrene transfer/cyclization,[9] and Toste's chiral anion phase transfer of aryldiazonium cations.[10]

Bromopyrroloindoline derivatives also serve as a privileged scaffold to access complex pyrroloindoline motifs bearing C3−N functionalization. For example, Rainier and co-workers used a Favorskii-like approach that benefits from anchimeric assistance from the methyl ester to provide robust access to this bond; Rainier's lab[11,12] and others have employed this strategy in the synthesis of kapakahines, pestalazine B, and other natural products bearing C3−N1′ bond.[13−17] Alternatively, functionalization of bromopyrroloindoline can result via a benzylic cation, which is then readily trapped with an appropriate nitrogen source.[18] For example, Movassaghi and co-workers reported a general strategy to build this C3−N1′ bond in the total synthesis of asperazine A and pestalazine B with stoichiometric Ag^{I} salts that proceeded through this benzylic cation.[19]

Motivated by the importance of the pyrroloindoline scaffold to the natural product and medicinal chemistry fields and the need to develop methods using earth-abundant metal and green solvents, we envisioned a disconnection that proceeded through a benzylic radical. We were drawn to the potential use of bromopyrroloindoline derivatives because they can be prepared on multigram scales in few high-yielding steps and the stereochemistry of the pyrroloindoline scaffold can be used to control the C3−N stereochemistry, providing a good platform from which to construct natural products. Moreover, direct C−C bond coupling of a pyrroloindoline-derived radical

Received: April 19, 2022
Published: July 25, 2022

https://doi.org/10.1021/acs.joc.2c00923
J. Org. Chem. 2022, 87, 9907−9914

Scheme 1. (A) Selected Examples of C3−N Pyrroloindoline Natural Products and (B) Our Approach to Indoline C3 Amination Proceeds via a Radical Intermediate

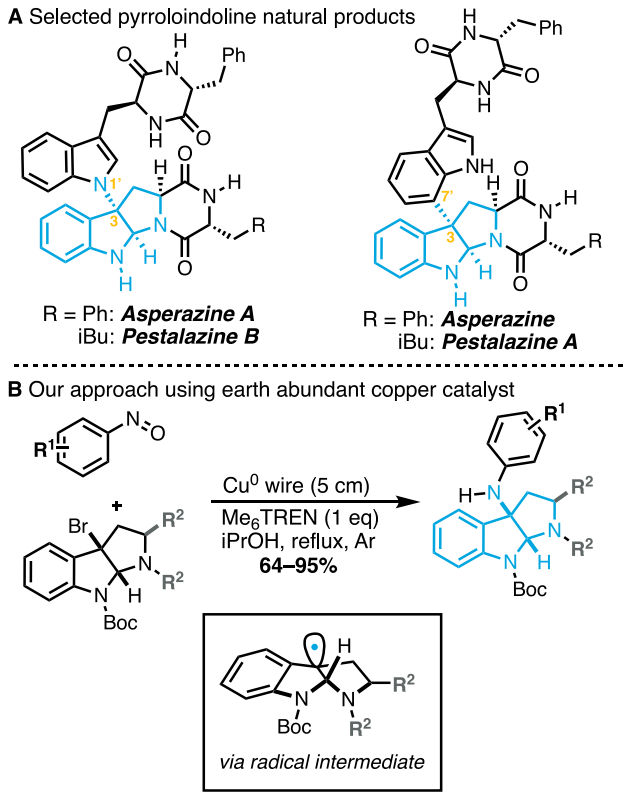

with substituted indole has been demonstrated using visible-light photoredox catalysis[20] and radical−radical coupling,[21−23] as well as copper-catalyzed radical cyclization to access 3-hydroxypyrroloindoline.[24] With this in mind and given our interest in copper-promoted nitrogen bond-forming reactions using nitroso derivatives,[25−27] we hypothesized that bromopyrroloindoline-based starting materials could be reduced by an electron-rich copper species to afford a carbon-centered radical that could then subsequently add into a nitrosoarene, furnishing the desired C3−N bond. After termination of the stable aminoxyl intermediate with a second equivalent of the indoline radical, reduction of the newly formed N−O dimerized intermediate would afford our desired aminated product (Scheme 2).

Herein, we report the realization of the above goals with the development of a robust and highly efficient approach for the installation of C3−amine bonds onto brominated pyrroloindoline scaffolds (Scheme 1B). The single-electron nature of our new method allows for facile installation of aniline motifs, regardless of their steric or electronic profiles. This approach employs propanol and other alcohols as green solvents[28−31] and a reusable earth-abundant copper metal to promote the reaction. To highlight the potential of this new approach, we demonstrate its use in the synthesis of a wide range of biologically relevant pyrrolodindoline and furoindoline scaffolds. Additionally, we describe an efficient eight-step total synthesis of (+)-asperazine A using this method, which includes a gram-scale synthesis of the key C−N bond-forming reaction.

RESULTS AND DISCUSSION

Our investigations began with amination on the tryptamine-derived scaffold **1** using our previously developed amination conditions (Table 1, entry 1).[25−27] Unfortunately, these conditions resulted in low yields (20%) and low conversion on this scaffold, with significant amounts of unreacted bromopyrroloindoline recovered after the reaction. To our surprise, however, we observed direct conversion to the aniline product without the formation of our hypothesized N−O dimer adduct (Scheme 2). Encouraged by the direct formation of the aniline-functionalized pyrrolodindoline **2**, we next explored conditions more similar to those used in the ATRP synthesis of low dispersity polymers.[32] Superstoichiometric zerovalent copper powder with catalytic Cu^{II} salts afforded the desired aniline in high yields (Table 1, entry 2). Switching the solvent from benzene to acetonitrile led to a significant decrease in yield (Table 1, entry 3). In acetonitrile, encouraging yields could be recovered by removing the Cu^{II} co-catalyst (Table 1, entry 4). Decreasing the equivalents of Cu powder improved the isolated yields (up to 81%); however, very low reproducibility was noted over four replicates (Table 1, entry 5). In this case, significant amounts of starting material were observed, indicating poor benzyl bromide activation.

We speculated that the lack of reproducibility and low conversion in this reaction may be a result of copper oxides at the surface of the powder. Presumably, this could be addressed using a higher purity level of the copper powder source. However, inspired by practices common in ATRP synthesis,[33−36] we moved toward the use of copper wire wrapped stir bar as the zerovalent copper source. Washing the wire with concentrated HCl immediately prior to use in the reaction provides a facile method to access an "active" copper surface. Moreover, we were able to reuse the same copper wire wrapped stir bar with no significant change in the reaction's isolated yield, indicating that this reaction does not foul the copper surface and only a fraction of the 5.5 equiv from the 5 cm wire is being consumed (Figure 1). Additionally, comparable yields were obtained using a slightly decreased

Scheme 2. Our Originally Hypothesized Product and Reaction Pathway[a]

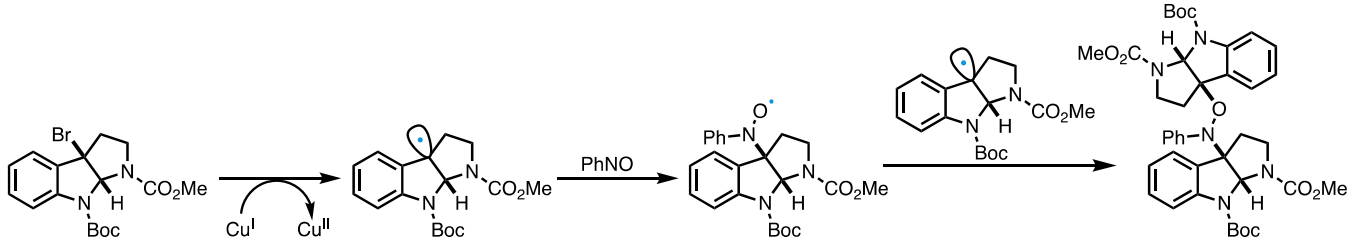

[a]Note, our newly proposed scheme deviates at the aminoxyl radical step.

https://doi.org/10.1021/acs.joc.2c00923
J. Org. Chem. 2022, 87, 9907−9914

Table 1. Optimization of General Conditions[a]

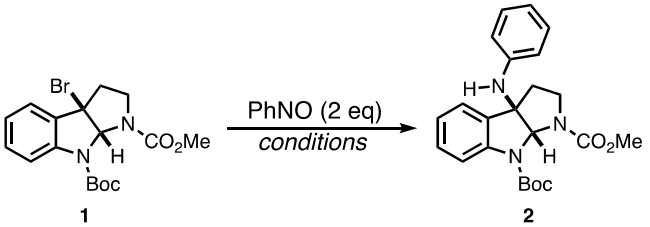

entry	solvent (temp)	ligand (equiv)	copper source	yield (%)
1	THF (35 °C)	PMDTA (1.5 equiv)	CuBr (1.1 equiv)	20
2	benzene (75 °C)	^{tbu}bpy (0.5 equiv)	Cu^0 powder (15 equiv), $Cu(OTf)_2$ (0.1 equiv)	77
3	MeCN (75 °C)	^{tbu}bpy (0.5 equiv)	Cu^0 powder (15 equiv), $Cu(OTf)_2$ (0.1 equiv)	56
4	MeCN (75 °C)	^{tbu}bpy (0.5 equiv)	Cu^0 powder (15 equiv)	76
5	MeCN (75 °C)	^{tbu}bpy (0.5 equiv)	Cu^0 powder (7 equiv)	65 ± 24
6	MeCN (75 °C)	^{tbu}bpy (0.5 equiv)	Cu^0 wire (5.5 equiv)	59
7	MeCN (75 °C)	PMDTA (0.5 equiv)	Cu^0 wire (5.5 equiv)	60
8	MeCN (75 °C)	PMDTA (1.0 equiv)	Cu^0 wire (5.5 equiv)	66
9	iPrOH (reflux)	PMDTA (1.0 equiv)	Cu^0 wire (5.5 equiv)	70
10[b]	iPrOH (reflux)	PMDTA (1.0 equiv)	Cu^0 wire (3.3 equiv)	68
11	**iPrOH (reflux)**	**Me_6TREN (1.0 equiv)**	**Cu^0 wire (5.5 equiv)**	84 ± 2
12	iPrOH (reflux)	Me_6TREN (1.0 equiv)	Cu^0 wire (5.5 equiv), $CuBr_2$ (0.1 equiv)	77
13[c]	**iPrOH (reflux)**	**Me_6TREN (1.0 equiv)**	**standard US Penny**	77

[a]Conditions with zerovalent Cu wire employed 5 cm of copper wire (5.5 equiv) wrapped around a stir bar, which was briefly cleaned with HCl immediately prior to use in the reaction. All yields are isolated yields and, unless indicated, all reaction times are 16 h. All entries were conducted with 25 mg of **1**. [b]Reaction was run for 36 h. [c]1 g scale of **1**.

amount of 5 cm copper wire, which is equivalent to 5.5 molar equiv vs 7 equiv of copper powder (Table 1 entries 5 and 6). Beyond observing acceptable yields with the copper wire conditions (Table 1, entry 6), the reaction was noticeably cleaner when analyzed by thin-layer chromatography (TLC) and no residual starting material was observed. Although moving from bipyridyl to the more activating PMDTA ligand led to an insignificant increase in isolated yields (Table 1, entries 6−7), increased ligand concentration and the use of refluxing isopropanol significantly improved the yields (Table 1, entries 8−9). Decreased copper loadings of 3 centimeters, or 3.3 molar equiv, provided similar yields to those of higher loadings, albeit with longer reaction times (Table 1, entry 10). Use of the more active Me_6TREN ligand afforded quantitative conversion when observed by ^{1}H NMR spectroscopy, excellent isolated yields, and extremely high reproducibility over five replicate reactions (Table 1, entry 11). No further improvement was observed with the addition of catalytic Cu^{II} salts (Table 1, entry 12). To highlight the robustness of this reaction, the 1-gram scale reaction was performed with a standard US penny similarly washed with an HCl solution (Table 1, entry 13). With optimized conditions in hand (Table 1, entry 11), we also investigated the scalability of this reaction beginning with 0.06 mmol (25 mg) of **1**. We found that scaling the reaction to 100 mg, 300 mg, and 1 g of **1** gave yields similar to and in some cases better than those at the 0.06 mmol scale (see SI, Table 1).

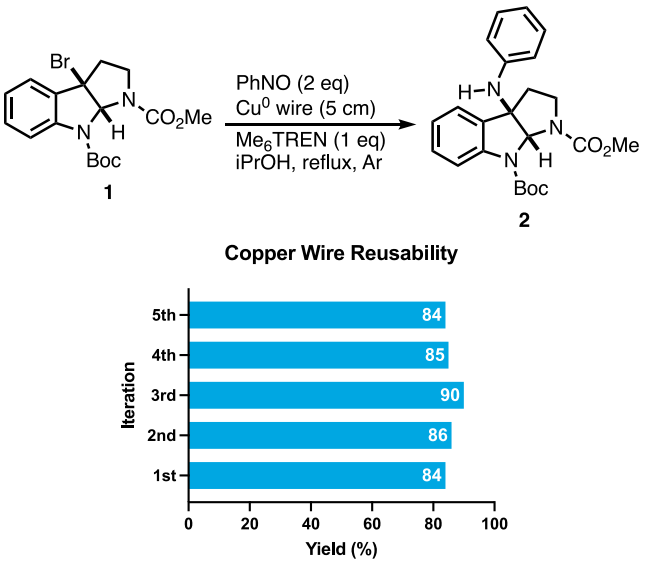

Figure 1. Five iterative reactions with the same copper wire, no significant reduction in yield is observed. Prior to each reaction, the copper wire wrapped stir bar is washed with conc. HCl. Reaction was run on a 0.06 mmol scale in each reaction.

To demonstrate the generality of the new method, we explored a series of electron-rich and -poor nitrosoarene coupling partners (Figure 2). Initial studies focused on electron-rich nitrosoarenes because current methods struggle with the construction of these motifs.[5,6] Our previous experience with radical nitrosoarene couplings led us to believe that a single-electron approach should perform well with these substrates. To our gratification, the electron-donating methoxy moiety is tolerated in the *ortho*-, *meta*-, and *para*-positions (**4**−**6**). Similar high yields were observed for the phenyl ether **8**, the strongly donating dimethylamino moiety **9**, and the thiomethyl substrate **10**. Encouraged by these results, we explored electron-deficient nitrosoarenes. Nitrile and ester functionalities were well supported in the *para*- and *meta*-positions (**11**−**14**). Nitrosoarenes functionalized with halogens were also well tolerated in the ortho-position and *para*-position (**15** and **16**). The *ortho*-iodo substrate **15** was isolated in high yield, indicating that no Ullman-type couplings had occurred. As Baran and others have demonstrated, the *ortho*-iodo derivative **15** can serve as the precursor to the indole unit found in the natural products via a Larock indole synthesis.[5−7,37,38] Sterically hindered nitrosoarenes were also well tolerated, as exemplified by the *o*-isopropyl nitrosoarene adduct **17**. Interestingly, nitrile and ester were not tolerated in the *ortho*-position, potentially due to the proximity of the intermediate aminoxyl radical that may react with these functional groups through an intramolecular addition reaction. In spite of these two examples, Figure 2 demonstrates the versatility of using our single-electron approach to construct sterically hindered C3−N indoline bond in excellent yields, regardless of steric or electronic substituents of the nitrosoarene.

https://doi.org/10.1021/acs.joc.2c00923
J. Org. Chem. 2022, 87, 9907−9914

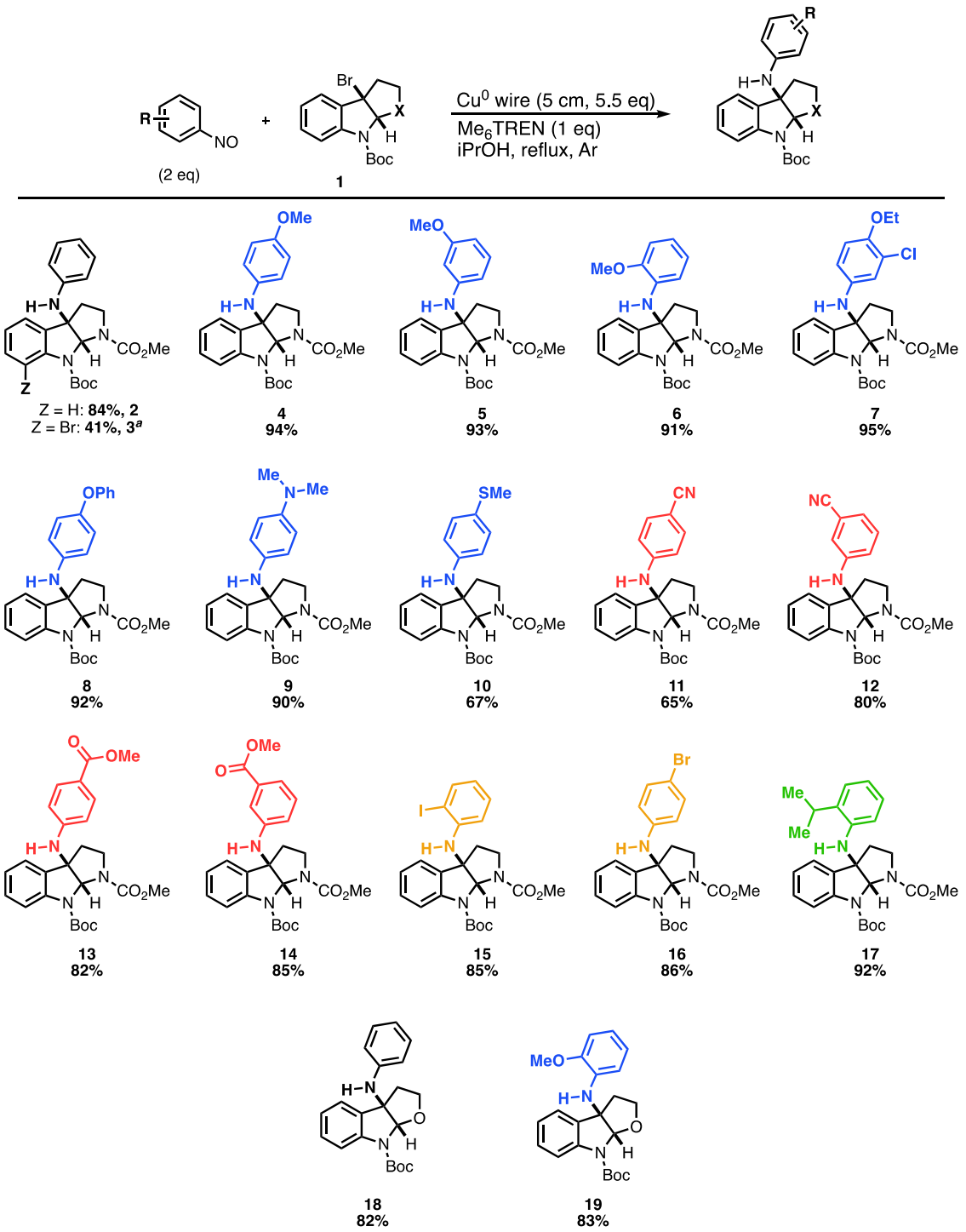

Figure 2. Substrate scope of pyrroloindolines and furoindoline using optimized conditions. [a]Reaction run at 45 °C.

Finally, to test the applicability of this method beyond pyrroloindolines, we explored the related furoindoline scaffolds (**18** and **19**), which can be found in a number of biologically active natural products and therapeutics. To our surprise, applying our optimized conditions toward brominated furoindolines yielded a significant amount of N−O dimer with our desired product. The corresponding N−O dimer was not observed in reactions using the related pyrrolodindolines, thus suggesting that the electronics or sterics of these scaffolds play a role in the lifetime and reactivity of the transient radical intermediates. Because we wanted to avoid the formation of the N−O dimer that requires an additional reduction step to afford the desired product, we modified the conditions slightly to favor access to **18**. Controlled addition of the brominated indoline **S9** dropwise over 90 min to the reaction solution effectively avoided dimerization of the starting materials when furoindoline scaffolds were used.

To further showcase the power of our methodology, we chose to synthesize a diketopiperazine **S15** (core molecule shown in Figure 3, **24**−**27**), which could serve as an intermediate in a potential total synthesis of chetomin. Interestingly, we found that upon reaction with our standard

https://doi.org/10.1021/acs.joc.2c00923
J. Org. Chem. 2022, 87, 9907−9914

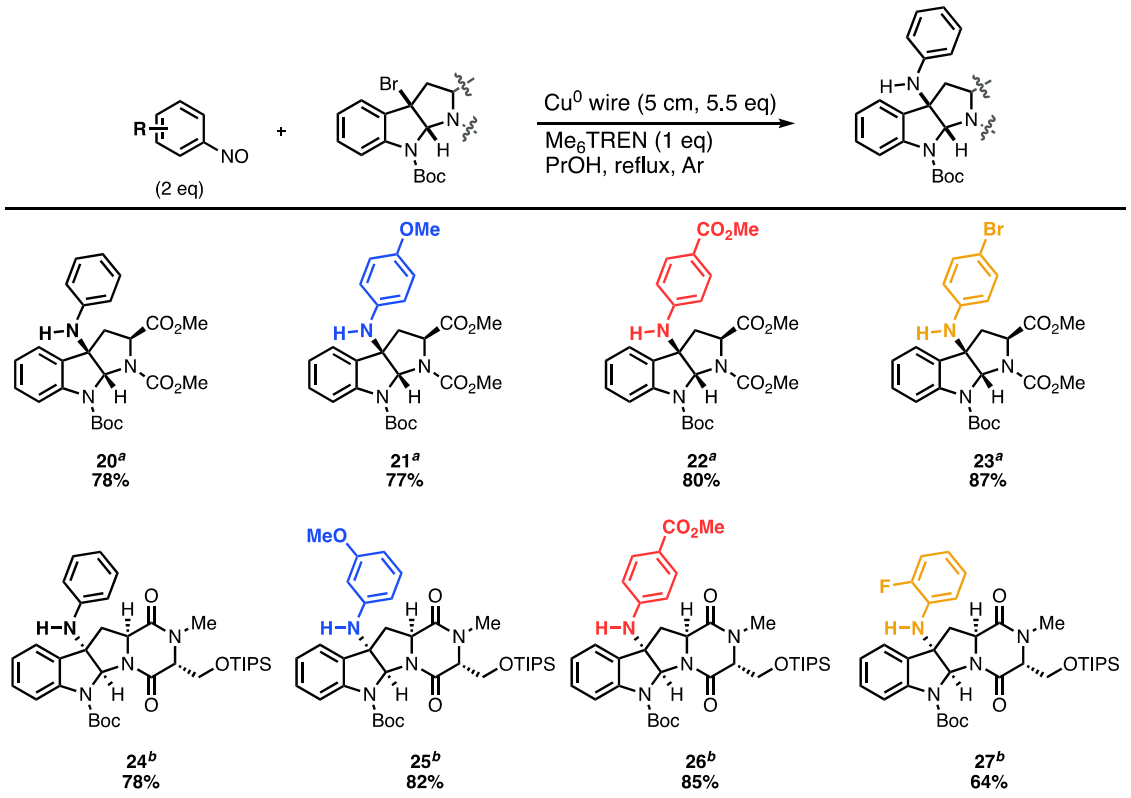

Figure 3. Scope of elaborated indoline substrates. [a]Reaction run in *i*-PrOH. [b]Reaction run in *n*-PrOH.

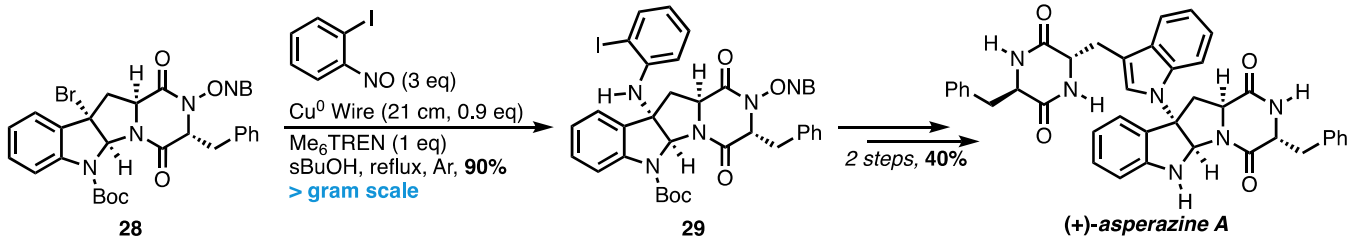

Figure 4. Key step in an eight-step total synthesis of (+)-asperazine A. ONB = *ortho*-nitrobenzyl.

conditions, a significant amount of the phenylhydroxylamine intermediate **IV** (Figure 5C) remained after up to 8 h at reflux (*vide infra*). However, simply changing the solvent from 2-propanol (b.p. 82 °C) to 1-propanol (b.p. 98 °C) gave faster conversion to the aniline product and thus a significantly cleaner reaction for the diketopiperazine scaffold. Once again, this scaffold could support functionalization with nitrosoarenes bearing diverse electronics (**24**−**27**). Having demonstrated an excellent scope of nitroso adducts, we next set out to demonstrate the applicability of this method for use on scaffolds that bore similarity to an advanced-stage natural product, including tryptophan-derived pyrroloindolines and diketopiperazine (Figure 3). Many successful natural product total syntheses employed a tryptophan-derived-brominated pyrroloindoline; after installing the desired C−N bond in a key step, the protected tryptophan carboxylic acid was subsequently functionalized to afford the natural product.[11−16,18,19] To our gratification, as with the model substrate, we found that the tryptophan-derived pyrroloindoline scaffold was compatible with a wide range of nitrosoarenes with diverse electronics, including electron neutral (**20**), rich (**21**), and poor (**22**) and a halide (**23**) functionalized nitrosoarenes for further downstream cross-coupling functionalization. Importantly, the compatibility of diketopiperazine scaffold (Figure 3, **24**−**27**) verifies the mildness of this method and sets the stage for the synthesis of natural products such as chetomin and asperazine A (*vide infra*).

Spurred by the success of these conditions on elaborated scaffolds, we sought to demonstrate the applicability of this method as a late-stage key step in the total synthesis of (+)-asperazine A. We chose asperazine A as a target due to its complex diketopiperazine fragment, crowded C3−N1′ fusion, and its multiple stereocenters. Further, in contrast to other C3−N1′ alkaloid natural products, there is only one total synthesis of asperazine A to date; we imagined our methodology would allow for a more concise synthesis.[19] Small-scale coupling studies with substrate **28** indicated that, while the use of both *i*-PrOH and *n*-PrOH as solvents afforded primarily a hydroxylamine intermediate similar to **IV**, *s*-BuOH provided **29** with high yields and scalability. To our delight, a gram-scale coupling of bromo-indoline **28** with 2-iodo-nitrosobenzene gave the desired iodoaniline product (**29**) in 90% yield (Figure 4). This material can be easily converted to (+)-asperazine A via a Larock heteroannulation, affording the natural product in 15% over eight steps from L-tryptophan (for full synthetic sequence, see the SI, Figure S1). Of note, to facilitate an

https://doi.org/10.1021/acs.joc.2c00923
J. Org. Chem. 2022, 87, 9907−9914

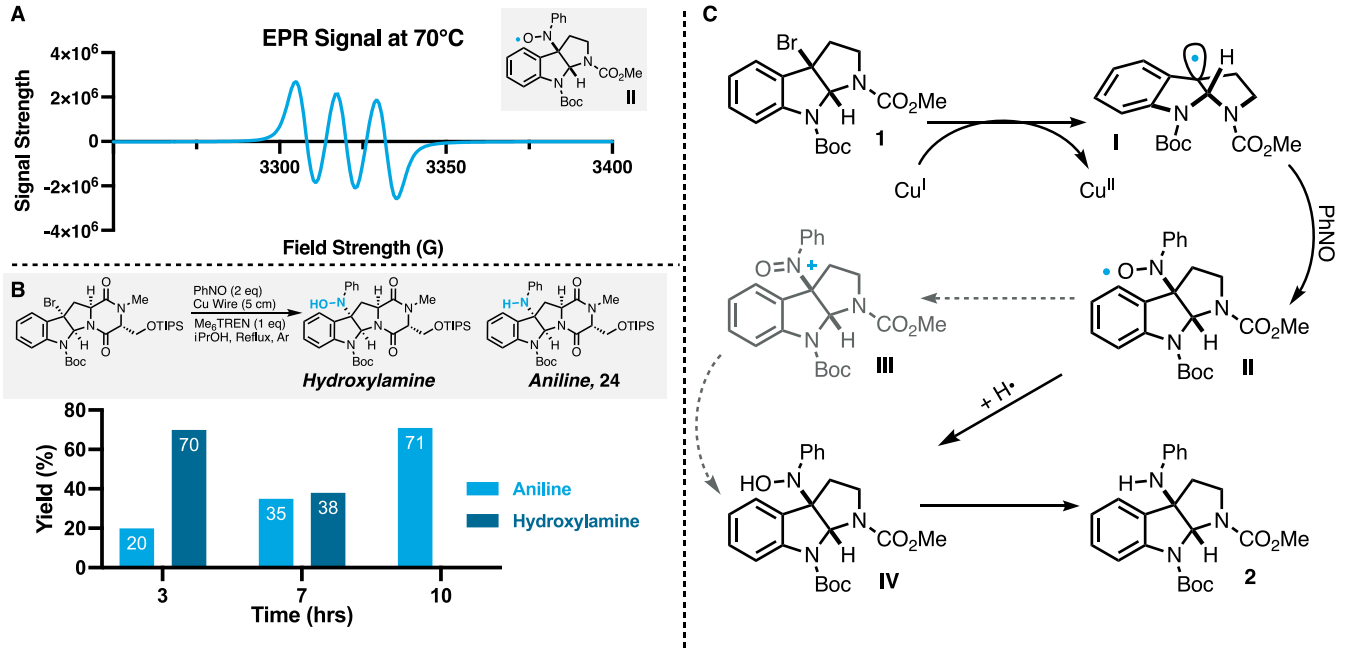

Figure 5. Key findings from mechanistic studies. (A) Observation of three equal resonances by EPR spectroscopy confirms the formation of an aminoxyl radical intermediate. (B) Loss of the hydroxylamine intermediate over time occurs with a concomitant increase in the aniline product. (C) Our proposed mechanism for this transformation. After Cu^{I}-mediated reduction of the carbon−bromine bond, radical addition forms aminoxyl intermediate (**II**). H-atom abstraction forms hydroxylamine (**IV**), which is reduced under reaction conditions to the desired product. Intermediates **I**, **II**, and **IV** were observed either directly via spectroscopy or through chemical derivatization.

efficient total synthesis, we found it was necessary to protect the amide hydrogen of the diketopiperazine ring. Without protection, low yields (32%) of the product were obtained as well as large amounts of unreacted starting material (>50%). After several protecting group strategies were evaluated, including Boc, PMB, and MOM protection, we identified that the photolabile *ortho*-nitrobenzyl group (ONB) was optimal for facilitating the key C3−N bond formation as well as for ease of deprotection. Our approach offers an efficient route to asperazine A but it also holds the potential to access other diketopiperazine natural products such as (+)-pestalazine B and chetomin.

With a thorough demonstration of the scope and synthetic applications completed, we next sought to investigate the reaction's mechanism. Because we did not observe an N−O dimer in most cases, we speculated that the reaction's mechanism must deviate from that of our previous work. Our first step in probing the mechanism of this transformation was to verify that we were indeed proceeding through a carbon-centered radical at the C3 position. The replacement of nitrosobenzene with the radical trapping agent TEMPO provided the corresponding TEMPO adduct (**S47**) in 82%, a yield similar to those with nitrosobenzene. This observation directly implicates carbon-centered radical **I** as a mechanistic intermediate. Next, we sought to verify the presence of an intermediate aminoxyl radical. Perpendicular-mode X-band electron paramagnetic resonance (EPR) spectra were collected on a Bruker EMX EPR spectrometer of our reaction running in an EPR tube at 70 °C. The EPR spectrum in Figure 5A shows three equal resonances, which is consistent with a coupling of an $S = 1/2$ spin to an $I = 1$ spin (14N), typical of the well-studied aminoxyl radical.[39] For definitive evidence of an aminoxyl-based radical, the spectrum was simulated and fit using EasySpin software.[40] The fitting parameters consisted of standard g and A parameters for an aminoxyl radical as a starting point and a Heisenberg exchange constant of 14.4212 MHz.[41] Finally, we investigated the role of the previously observed hydroxylamine in this mechanism to evaluate whether or not this was a possible intermediate. As described earlier, we observed the formation of hydroxylamine intermediate when we initially investigated the diketopiperazine derivative **24**. Using this transformation as a model system, we ran three reactions in parallel and recorded the isolated yields at various time points. As shown in Figure 5B, we observed a decreasing amount of hydroxylamine with a concomitant increase in the yield of aniline **24** as the reaction progressed. This observation indicates that the hydroxylamine is formed en route to the desired product **24**.

These observations lead us to the proposed mechanism in Figure 5C. Initially, a Cu^{I} species derived from the oxidation of copper wire reduces the C3 carbon−bromine bond to the corresponding benzylic-type radical **I**, generating Cu^{II} in the process. Radical addition into the nitroso-nitrogen forms aminoxyl intermediate **II** before H-atom transfer forms hydroxylamine **IV**, which is subsequently reduced to the desired aniline **2**. Literature evidence suggests that in secondary alcohol solvents, the aminoxyl radical intermediate **II** may proceed to the hydroxylamine **IV** by way of an oxoammonium-like intermediate **III**; oxidation of the solvent by **III** would yield **IV**.[42,43] Other pathways for H-atom transfer are also likely involved; however, this transformation also proceeds with acetonitrile and benzene (Table 1, entries 1 and 8). This is not unique to the pyrroloindoline-based scaffolds, as this reactivity is also observed with related furoindoline scaffolds (albeit to a lesser extent). However, it is clear that the structure of the radical precursor plays a vital role in the efficiency of this process. Efforts are ongoing to elucidate the nature of the H-atom transfer, which forms hydroxylamine **IV**,

https://doi.org/10.1021/acs.joc.2c00923
J. Org. Chem. 2022, 87, 9907−9914

as well as the means of the conversion of **IV** to anilines such as **2**.

CONCLUSIONS

In conclusion, we have developed a single electron-based method for the direct installation of aryl C3−N linkages onto C3-brominated pyrroloindoline and furoindoline scaffolds. By leveraging a single-electron pathway, we are able to functionalize our desired scaffolds with excellent yields under mild conditions with a wide range of relevant functionality, irrespective of steric or electronic nature of the aryl nitroso derivative. These substrates are of interest to the medicinal chemistry and natural product synthesis communities. We have further demonstrated the applicability of this new method with a concise eight-step total synthesis of (+)-asperazine A. Future investigations will explore the development of other bond-forming processes that employ earth-abundant copper metal catalysts and green alcohol solvents.

ASSOCIATED CONTENT

Supporting Information

The Supporting Information is available free of charge at https://pubs.acs.org/doi/10.1021/acs.joc.2c00923.

Experimental details, materials, methods, characterization data of products, ^{1}H and ^{13}C NMR spectra for all compounds (PDF)

AUTHOR INFORMATION

Corresponding Author

Javier Read de Alaniz − *Department of Chemistry and Biochemistry, University of California at Santa Barbara, Santa Barbara, California 93106, United States;* orcid.org/0000-0003-2770-9477; Email: javier@chem.ucsb.edu

Authors

James B. Shaum − *Department of Chemistry and Biochemistry, University of California at Santa Barbara, Santa Barbara, California 93106, United States*

Andrei Nikolaev − *Department of Chemistry and Biochemistry, University of California at Santa Barbara, Santa Barbara, California 93106, United States*

Helena C. Steffens − *Department of Chemistry and Biochemistry, University of California at Santa Barbara, Santa Barbara, California 93106, United States*

Luis Gonzalez − *Department of Chemistry and Biochemistry, University of California at Santa Barbara, Santa Barbara, California 93106, United States*

Shamon Walker − *Materials Department and Materials Research Laboratory, University of California at Santa Barbara, Santa Barbara, California 93106, United States*

Andrey V. Samoshin − *Department of Chemistry and Biochemistry, University of California at Santa Barbara, Santa Barbara, California 93106, United States*

Gabrielle Hammersley − *Department of Chemistry and Biochemistry, University of California at Santa Barbara, Santa Barbara, California 93106, United States*

Ellia H. La − *Department of Chemistry and Biochemistry, University of California at Santa Barbara, Santa Barbara, California 93106, United States*

Complete contact information is available at: https://pubs.acs.org/10.1021/acs.joc.2c00923

Author Contributions

J.B.S., A.N., H.C.S., and L.G. designed the experiments and performed and analyzed the experimental results. A.V.S., G.H., and E.H.L. conducted the initial stages of the method optimization. S.W. conducted the electron paramagnetic resonance (EPR) experiments and analysis in this work. J.B.S. and J.R.d.A. wrote the paper with input from the other co-authors.

Notes

The authors declare no competing financial interest.

ACKNOWLEDGMENTS

The authors thank the National Science Foundation (CHE-1566614) for financial support. This work utilized NMR instruments supported by the National Science Foundation under award No. MRI-1920299. Mass spectrometry instrumentation was partially supported by the MRL Shared Experimental Facilities, which are supported by the MRSEC Program of the NSF (DMR-1121053).

REFERENCES

(1) Ruiz-Sanchis, P.; Savina, S. A.; Albericio, F.; Álvarez, M. Structure, Bioactivity and Synthesis of Natural Products with Hexahydropyrrolo[2,3-b]Indole. *Chem.−Eur. J.* **2011**, *17*, 1388−1408.

(2) Staab, A.; Loeffler, J.; Said, H. M.; Diehlmann, D.; Katzer, A.; Beyer, M.; Fleischer, M.; Schwab, F.; Baier, K.; Einsele, H.; Flentje, M.; Vordermark, D. Effects of HIF-1 Inhibition by Chetomin on Hypoxia-Related Transcription and Radiosensitivity in HT 1080 Human Fibrosarcoma Cells. *BMC Cancer* **2007**, *7*, 213.

(3) Schallenberger, M. A.; Newhouse, T.; Baran, P. S.; Romesberg, F. E. The Psychotrimine Natural Products Have Antibacterial Activity against Gram-Positive Bacteria and Act via Membrane Disruption. *J. Antibiot.* **2010**, *63*, 685−687.

(4) Repka, L. M.; Reisman, S. E. Recent Developments in the Catalytic, Asymmetric Construction of Pyrroloindolines Bearing All-Carbon Quaternary Stereocenters. *J. Org. Chem.* **2013**, *78*, 12314−12320.

(5) Newhouse, T.; Baran, P. S. Total Synthesis of (±)-Psychotrimine. *J. Am. Chem. Soc.* **2008**, *130*, 10886−10887.

(6) Newhouse, T.; Lewis, C. A.; Eastman, K. J.; Baran, P. S. Scalable Total Syntheses of N-Linked Tryptamine Dimers by Direct Indole−Aniline Coupling: Psychotrimine and Kapakahines B and F. *J. Am. Chem. Soc.* **2010**, *132*, 7119−7137.

(7) Newhouse, T.; Lewis, C. A.; Baran, P. S. Enantiospecific Total Syntheses of Kapakahines B and F. *J. Am. Chem. Soc.* **2009**, *131*, 6360−6361.

(8) Gentry, E. C.; Rono, L. J.; Hale, M. E.; Matsuura, R.; Knowles, R. R. Enantioselective Synthesis of Pyrroloindolines via Noncovalent Stabilization of Indole Radical Cations and Applications to the Synthesis of Alkaloid Natural Products. *J. Am. Chem. Soc.* **2018**, *140*, 3394−3402.

(9) Zhang, G.-Y.; Peng, Y.; Xue, J.; Fan, Y.-H.; Deng, Q.-H. Copper-Catalyzed Nitrene Transfer/Cyclization Cascade to Synthesize 3a-Nitrogenous Furoindolines and Pyrroloindolines. *Org. Chem. Front.* **2019**, *6*, 3934−3938.

(10) Nelson, H. M.; Reisberg, S. H.; Shunatona, H. P.; Patel, J. S.; Toste, F. D. Chiral Anion Phase Transfer of Aryldiazonium Cations: An Enantioselective Synthesis of C3-Diazenated Pyrroloindolines. *Angew. Chem., Int. Ed.* **2014**, *53*, 5600−5603.

(11) Espejo, V. R.; Rainier, J. D. An Expeditious Synthesis of C(3)−N(1′) Heterodimeric Indolines. *J. Am. Chem. Soc.* **2008**, *130*, 12894−12895.

(12) Espejo, V. R.; Rainier, J. D. Total Synthesis of Kapakahine E and F. *Org. Lett.* **2010**, *12*, 2154−2157.

(13) Pérez-Balado, C.; de Lera, Á. R. Concise Total Synthesis and Structural Revision of (+)-Pestalazine B. *Org. Biomol. Chem.* **2010**, *8*, 5179−5186.

(14) Welch, T. R.; Williams, R. M. Studies on the Biosynthesis of Chetomin: Enantiospecific Synthesis of a Putative, Late-Stage Biosynthetic Intermediate. *Tetrahedron* **2013**, *69*, 770−773.
(15) Horibe, T.; Ohmura, S.; Ishihara, K. Selenium−Iodine Cooperative Catalyst for Chlorocyclization of Tryptamine Derivatives. *Org. Lett.* **2017**, *19*, 5525−5528.
(16) Gallego, S.; Lorenzo, P.; Alvarez, R.; de Lera, A. R. Total Synthesis of Naturally Occurring (+)-Psychotriasine and the Related Tetrahydro-*β*-Carboline, Dimeric Tryptamines with NC Connectivities. *Tetrahedron Lett.* **2017**, *58*, 210−212.
(17) Villanueva-Margalef, I.; Thurston, D. E.; Zinzalla, G. Facile Nucleophilic Substitution at the C3a Tertiary Carbon of the 3a-Bromohexahydropyrrolo[2,3-b]Indole Scaffold. *Org. Biomol. Chem.* **2010**, *8*, 5294−5303.
(18) Hakamata, H.; Ueda, H.; Tokuyama, H. Construction of Indole Structure on Pyrroloindolines via AgNTf2-Mediated Amination/Cyclization Cascade: Application to Total Synthesis of (+)-Pestalazine B. *Org. Lett.* **2019**, *21*, 4205−4209.
(19) Nelson, B. M.; Loach, R. P.; Schiesser, S.; Movassaghi, M. Concise Total Synthesis of (+)-Asperazine A and (+)-Pestalazine B. *Org. Biomol. Chem.* **2018**, *16*, 202−207.
(20) Furst, L.; Narayanam, J. M. R.; Stephenson, C. R. J. Total Synthesis of (+)-Gliocladin C Enabled by Visible-Light Photoredox Catalysis. *Angew. Chem., Int. Ed.* **2011**, *50*, 9655−9659.
(21) Lathrop, S. P.; Pompeo, M.; Chang, W.-T. T.; Movassaghi, M. Convergent and Biomimetic Enantioselective Total Synthesis of (−)-Communesin F. *J. Am. Chem. Soc.* **2016**, *138*, 7763−7769.
(22) Lindovska, P.; Movassaghi, M. Concise Synthesis of (−)-Hodgkinsine, (−)-Calycosidine, (−)-Hodgkinsine B, (−)-Quadrigemine C, and (−)-Psycholeine via Convergent and Directed Modular Assembly of Cyclotryptamines. *J. Am. Chem. Soc.* **2017**, *139*, 17590−17596.
(23) Lathrop, S. P.; Movassaghi, M. Application of Diazene-Directed Fragment Assembly to the Total Synthesis and Stereochemical Assignment of (+)-Desmethyl-Meso-Chimonanthine and Related Heterodimeric Alkaloids. *Chem. Sci.* **2014**, *5*, 333−340.
(24) Deng, X.; Liang, K.; Tong, X.; Ding, M.; Li, D.; Xia, C. Copper-Catalyzed Radical Cyclization to Access 3-Hydroxypyrroloindoline: Biomimetic Synthesis of Protubonine A. *Org. Lett.* **2014**, *16*, 3276−3279.
(25) Fisher, D. J.; Burnett, G. L.; Velasco, R.; Read de Alaniz, J. Synthesis of Hindered *α*-Amino Carbonyls: Copper-Catalyzed Radical Addition with Nitroso Compounds. *J. Am. Chem. Soc.* **2015**, *137*, 11614−11617.
(26) Fisher, D. J.; Shaum, J. B.; Mills, C. L.; Read de Alaniz, J. Synthesis of Hindered Anilines: Three-Component Coupling of Arylboronic Acids, Tert-Butyl Nitrite, and Alkyl Bromides. *Org. Lett.* **2016**, *18*, 5074−5077.
(27) Shaum, J. B.; Fisher, D. J.; Sroda, M. M.; Limon, L.; Read de Alaniz, J. Direct Introduction of Nitrogen and Oxygen Functionality with Spatial Control Using Copper Catalysis. *Chem. Sci.* **2018**, *9*, 8748−8752.
(28) Doble, M.; Kruthiventi, A. K. *Alternate Solvents*, In Doble, M.; Kruthiventi, A. K. B. T.-G. C.; E, Eds.; Academic Press: Burlington, 2007; Chapter 5, pp 93−104.
(29) Gupta, J.; Wilson, B. W.; Vadlani, P. V. Evaluation of Green Solvents for a Sustainable Zein Extraction from Ethanol Industry DDGS. *Biomass Bioenergy* **2016**, *85*, 313−319.
(30) Zhou, X.; Li, X. Catalyst-Free System for Sulfenylation of Free (N−H) Indoles with 2,2′-Dithiosalicylic Acid under Alkaline Conditions. *RSC Adv.* **2014**, *4*, 1241−1245.
(31) Jang, J.; Nam, Y. T.; Kim, D.; Kim, Y.-J.; Kim, D. W.; Jung, H.-T. Turbostratic Nanoporous Carbon Sheet Membrane for Ultrafast and Selective Nanofiltration in Viscous Green Solvents. *J. Mater. Chem. A* **2020**, *8*, 8292−8299.
(32) Matyjaszewski, K. Atom Transfer Radical Polymerization (ATRP): Current Status and Future Perspectives. *Macromolecules* **2012**, *45*, 4015−4039.
(33) Magenau, A. J. D.; Kwak, Y.; Matyjaszewski, K. ATRP of Methacrylates Utilizing CuIIX2/L and Copper Wire. *Macromolecules* **2010**, *43*, 9682−9689.
(34) Boyer, C.; Corrigan, N. A.; Jung, K.; Nguyen, D.; Nguyen, T.-K.; Adnan, N. N. M.; Oliver, S.; Shanmugam, S.; Yeow, J. Copper-Mediated Living Radical Polymerization (Atom Transfer Radical Polymerization and Copper(0) Mediated Polymerization): From Fundamentals to Bioapplications. *Chem. Rev.* **2016**, *116*, 1803−1949.
(35) Urbani, C. N.; Bell, C. A.; Whittaker, M. R.; Monteiro, M. J. Convergent Synthesis of Second Generation AB-Type Miktoarm Dendrimers Using "Click" Chemistry Catalyzed by Copper Wire. *Macromolecules* **2008**, *41*, 1057−1060.
(36) St Amant, A. H.; Discekici, E. H.; Bailey, S. J.; Zayas, M. S.; Song, J-A.; Shankel, S. L.; Nguyen, S. N.; Bates, M. W.; Anastasaki, A.; Hawker, C. J.; Read de Alaniz, J. Norbornadienes: Robust and Scalable Building Blocks for Cascade ″Click″ Coupling of High Molecular Weight Polymers. *J. Am. Chem. Soc.* **2019**, *141*, 13619−13624.
(37) Li, Q.; Xia, T.; Yao, L.; Deng, H.; Liao, X. Enantioselective and Diastereoselective Azo-Coupling/Iminium-Cyclizations: A Unified Strategy for the Total Syntheses of (−)-Psychotriasine and (+)-Pestalazine B. *Chem. Sci.* **2015**, *6*, 3599−3605.
(38) Liu, C.; Yi, J.-C.; Zheng, Z.-B.; Tang, Y.; Dai, L.-X.; You, S.-L. Enantioselective Synthesis of 3a-Amino-Pyrroloindolines by Copper-Catalyzed Direct Asymmetric Dearomative Amination of Tryptamines. *Angew. Chem., Int. Ed.* **2016**, *55*, 751−754.
(39) Clark, A.; Sedhom, J.; Elajaili, H.; Eaton, G. R.; Eaton, S. S. Dependence of Electron Paramagnetic Resonance Spectral Lineshapes on Molecular Tumbling: Nitroxide Radical in Water:Glycerol Mixtures. *Concepts Magn. Reson. Part A* **2016**, *45A*, No. e21423.
(40) Stoll, S.; Schweiger, A. EasySpin, a Comprehensive Software Package for Spectral Simulation and Analysis in EPR. *J. Magn. Reson.* **2006**, *178*, 42−55.
(41) Bowman, P. B.; Puett, D. Electron Paramagnetic Resonance Spectroscopy of Nitroxide-Labeled Calmodulin. *Protein J.* **2014**, *33*, 267−277.
(42) Walroth, R. C.; Miles, K. C.; Lukens, J. T.; MacMillan, S. N.; Stahl, S. S.; Lancaster, K. M. Electronic Structural Analysis of Copper(II)−TEMPO/ABNO Complexes Provides Evidence for Copper(I)−Oxoammonium Character. *J. Am. Chem. Soc.* **2017**, *139*, 13507−13517.
(43) Badalyan, A.; Stahl, S. S. Cooperative Electrocatalytic Alcohol Oxidation with Electron-Proton-Transfer Mediators. *Nature* **2016**, *535*, 406−410.

https://doi.org/10.1021/acs.joc.2c00923
J. Org. Chem. 2022, 87, 9907−9914